Insights into Conformational Ensembles of Compositionally Identical Disordered Peptidomimetics

Erin C. Day, Keila C. Cunha, Jianhan Zhao, Audra J. DeStefano, James N. Dodds, Melissa A. Yu, Songi Han, Erin S. Baker, Joan-Emma Shea, Rebecca B. Berlow, Abigail S. Knight*

Department of Chemistry, The University of North Carolina at Chapel Hill, Chapel Hill, North Carolina 27599, United States.

Keywords: *peptoids, intrinsic disorder, conformation characterization, solvatochromic dye*

Abstract: While the conformational ensembles of disordered peptides and peptidomimetics are complex and challenging to characterize, they are a critical component in the paradigm connecting macromolecule sequence, structure, and function. In molecules that do not adopt a single predominant conformation, the conformational ensemble contains rich structural information that, if accessible, can provide a fundamental understanding related to desirable functions such as cell penetration of a therapeutic or the generation of tunable enzyme-mimetic architecture. To address the fundamental challenge of describing broad conformational ensembles, we developed a model system of peptidomimetics comprised of polar glycine and hydrophobic *N*-butylglycine to characterize using a suite of analytical techniques. Using replica exchange molecular dynamics atomistic simulations and liquid chromatography coupled to ion mobility spectrometry, we were able to distinguish the conformations of compositionally identical model sequences. However, differences between these model sequences were more challenging to resolve with characterization tools developed for intrinsically disordered proteins and polymers, including double electron-electron resonance (DEER) spectroscopy and diffusion ordered spectroscopy (DOSY) NMR. Finally, we introduce a facile colorimetric assay using immobilized sequences that leverages a solvatochromic probe, Reichardt's dye, to visually reveal conformational trends consistent with the experimental and computational analysis. This rapid colorimetric technique provides a complementary method to characterize the disorder of macromolecules and unravel the complexity of conformational ensembles as an isolated or multiplexed technique.

Introduction

Disordered oligomers play critical roles in natural systems of biomacromolecules, but their conformational complexity exists beyond the classical structure-function paradigm.[1–3] Highly-ordered biopolymers such as proteins, which access only a handful of conformations, are well-characterized with existing techniques such as crystallography and cryogenic electron microscopy, resulting in fundamental design principles connecting primary sequences with folded structures. However, the complex conformational and energetic landscapes of disordered biopolymers and synthetic oligomers are poorly understood (Figure 1a).[4] Establishing similar design principles for these materials demands techniques that can readily capture conformational dispersity. Currently, there are limited experimental strategies available to capture these distributions and enable sensitive detection of the subtle differences between compositionally identical macromolecules that differ only in sequence.[5–7] Developing sequence-structure and structure-function relationships for disordered macromolecules is essential for advancing next generation biomaterials and therapeutics.[6,8]

Current techniques have both advantages and limitations when implemented for the characterization of small (< 3 kDa) macromolecules (Figure 1b). Ensemble averaging can present a challenge for many methods utilized for characterization and comparison of small, disordered macromolecules with similar compositions. Synthetic polymers can be successfully characterized by dynamic light scattering and size exclusion chromatography, but these methods provide poor resolution for smaller scaffolds. Circular dichroism and infrared spectroscopies are compatible with smaller scaffolds; however, they only reveal secondary structure and cannot fully describe the structure of disordered oligomers that lack a chiral moiety or regions of local structure.[10,11] Solution NMR methods such as diffusion ordered spectroscopy (DOSY)[12] are capable of revealing conformational profiles of disordered macromolecules; however, these methods are time intensive and can require a prohibitive amount of material (> 0.5 mg). Ion mobility spectrometry (IMS) can probe small amounts of material; however, it has only recently been implemented in the characterization of macromolecular conformation.[13] Techniques that probe end-to-end distance, including double electron–electron resonance (DEER) spectroscopy, analyze a distribution of conformations; however, this can be time intensive and offer limited resolution outside of 2-9 nm.[14] Each effort at the frontier of analytical characterization can reveal unique descriptors of the conformational landscape but rarely capture its full extent. To supplement experimental characterization, atomistic simulations can provide detailed information about the conformational distribution but are computationally intensive.[15] Therefore, the pursuit of a comprehensive understanding of conformational complexities demands a diverse suite of characterization methods.

Peptoids, *N*-substituted glycine oligomers, serve as an excellent model scaffold for elucidating the complementary capabilities of conformational characterization techniques.[6,16] Peptoids can mimic the structure and function of proteins by adopting compact morphologies and secondary structures, enabling the development of functional materials including therapeutics,[17,18] catalysts,[19,20] devices encoding information,[21] and biomolecule receptors.[22–24] While peptoid sequences can form helices[25–28] and nanosheets[24,29], side-chains can be selected that do not form secondary structure,[1,30] allowing the isolation of variables such as hydrophobic[30,31] or charge patterning[28,32] and their impact on conformation.

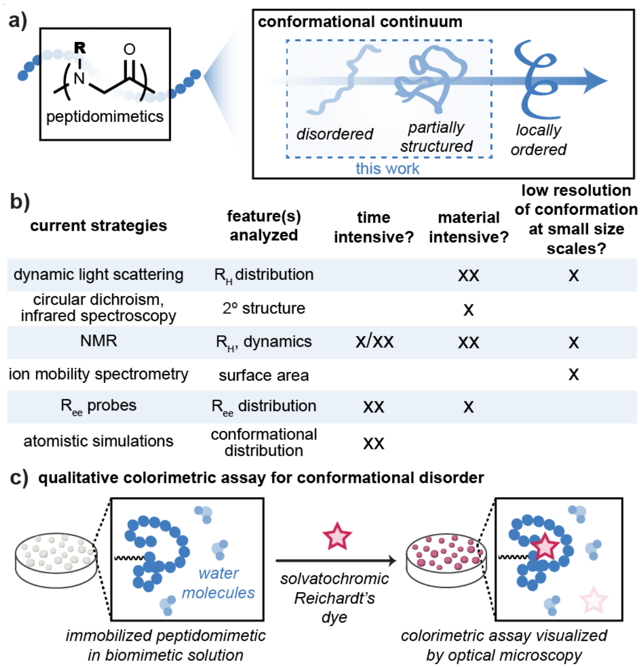

current strategies	feature(s) analyzed	time intensive?	material intensive?	low resolution of conformation at small size scales?
dynamic light scattering	R_H distribution		XX	X
circular dichroism, infrared spectroscopy	2° structure		X	
NMR	R_H, dynamics	X/XX	XX	X
ion mobility spectrometry	surface area			X
R_{ee} probes	R_{ee} distribution	XX	X	
atomistic simulations	conformational distribution	XX		

Figure 1. Overview of the continuum of disorder for peptidomimetics and methods for structural characterization. a) Scope of structural disorder of sequence-defined oligomers. b) Existing methods for characterizing small macromolecules. Time intensive techniques typically require > 20 min (X), > 2 h (XX); material intensive typically require > 10 µg (X), > 0.5 mg (XX); and small size scales refers to materials smaller than 3 kDa. c) Schematic of the colorimetric platform for characterizing structural disorder.

The conformational distribution of four peptoids with unique hydrophobic patterning is characterized herein using a combination of complementary computational and experimental techniques, including a versatile colorimetric assay. Atomistic simulations provide high-resolution insights, while experimentally, IMS, DOSY NMR, and DEER spectroscopy provide complementary insights into the peptoids' conformational distributions. To supplement existing structural characterization methods for disordered macromolecules, we developed a versatile colorimetric assay using a solvatochromic dye and broadly accessible instrumentation (Figure 1c). Solvatochromic dyes[33] have been used for various applications, such as staining hydrophobic regions in proteins[34] and intracellular lipid droplets,[35] visualizing molecular weight differences in supramolecular polymers,[36] in addition to characterizing the hydrophobic microenvironments of synthetic dendrimers,[37] surfaces,[38] single-[30,39] and multichain assemblies.[40–42] Our immobilized colorimetric assay similarly leverages the polarity responsiveness of a solvatochromic dye, Reichardt's dye, to visually reveal conformational differences. Our results corroborate differences observed by the aforementioned analytical techniques, ultimately enabling facile characterization of single-chain disorder and compactness of oligomeric sequences, adding a valuable tool to the characterization toolbox for complex conformational landscapes.

Results and Discussion

Design of model HP peptoids. We designed four peptoids with identical compositions and varied sequences to target conformational differences independent of composition (Figure 2a). Hydrophobic patterning has been demonstrated to yield differences in conformation with previous HP models where "H" describes a hydrophobic residue and "P" describes a polar residue in both experimental characterization with larger macromolecules (e.g., 100mers) and macromolecule simulations.[30,43–45] We selected *N*-butylglycine as the hydrophobic monomer and glycine as the polar residue. This system enables the isolation of one side-chain interaction, hydrophobic collapse, without extraneous variables such as charge or aromaticity. These residues were arranged into peptoids of 20 monomers in length (20mers; Figure 2a and S1), which are short enough to achieve high-purity syntheses and long enough to yield conformations with different degrees of disorder.[5,44,46] Two sequences at the extremes of the sequence space were selected: diblock (**dib**) and alternating (**alt**) (Figure 2a). These hydrophobicity patterns have demonstrated different properties, such as temperature-induced phase separation with thermoresponsive peptides in solution[47] and bulk interfacial width with a mixture of styrene-peptoid conjugates.[31] Two randomized sequences (**r1** and **r2**) were additionally selected to provide an intermediate number of hydrophobic blocks, considering the established role of hydrophobic patterning in macromolecular conformation.[30,48]

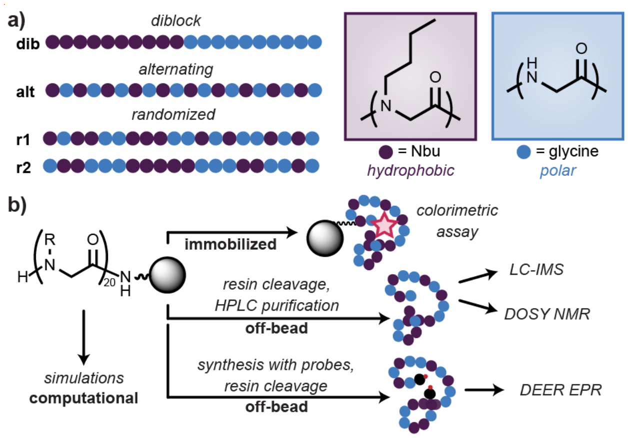

Figure 2. Sequence workflow and design. a) Schematic describing the 20mer peptidomimetics with identical compositions (left) and monomer structures (right): hydrophobic (*N*-butylglycine) and polar (glycine). b) Schematic describing use of solid-phase synthesis to prepare 20mers for characterization of disorder.

Macromolecules were synthesized using a combination of the submonomer method of peptoid synthesis[49] with a bromoacetic acid acylation followed by substitution with n-butylamine and traditional Fmoc-peptide synthesis to couple a protected glycine monomer (Figure 2b). The modular submonomer method also enabled synthesis of peptoids with site specific probes (i.e., residues with radical probes to facilitate characterization with DEER spectroscopy).

Atomistic simulations. Molecular dynamics (MD) simulations uniquely reveal atomic-level descriptions of the conformational distributions. Replica exchange MD allows a better exploration of the conformational space, and thus this technique was performed for each of the four peptoids. The force field used was an adaptation from GROMOS 53A6 that considers the conformations for peptoids.[50] Simulations of each peptoid as a single chain in bulk water (50,000 conformations of each peptoid) revealed distributions of radii of gyration, end-to-end distances, and numbers of hydrogen bonds (Figure 3a). Analysis of one peptoid molecule enabled single chain conformational analysis without the possibility of multichain assemblies or aggregation. In addition to the four peptoid sequences, we simulated a homoglycine 20mer (**gly$_{20}$**) as a control sequence lacking hydrophobic side-chains (Figure S1). The smallest average radius of gyration of the peptoid backbone [excluding side-chain contributions; $R_{g(bkb)}$] was observed for **alt** (0.62 nm) followed by **r1** (0.63 nm). Larger $R_{g(bkb)}$ values were calculated for **dib**, **r2**, and **gly$_{20}$**, all with an average of 0.65 nm (Figures 3a and S2, Table S1). Radii of gyration of the molecules including side-chain contributions showed fewer differences between the model sequences, which we hypothesize is due to the contribution of freely rotating butyl chains to the allocation of mass in the macromolecule. The R_g probability distribution for **gly$_{20}$** was wider than any of the four peptoids that contain hydrophobic residues (Figure S2).

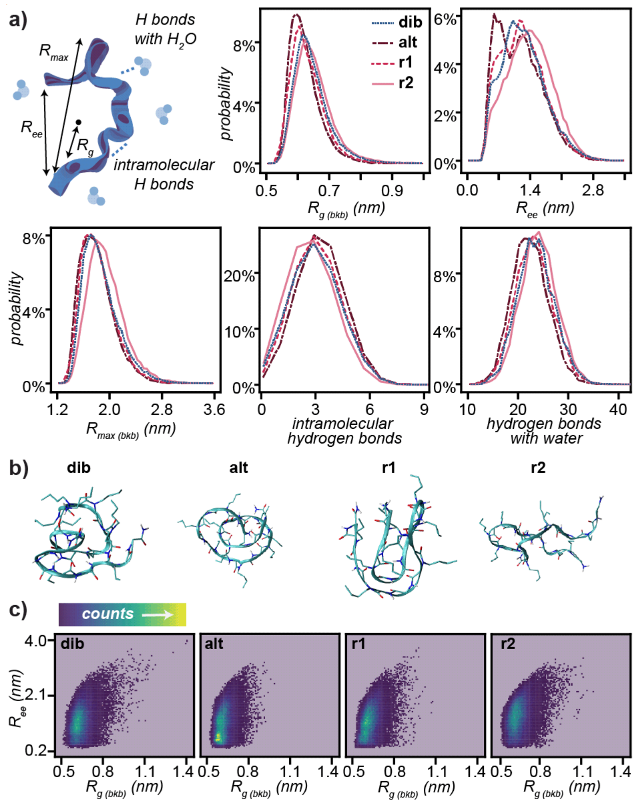

Figure 3. Simulation measurements. a) Schematic of measurements extracted from simulations (top left). Normalized probability distributions of radius of gyration (backbone only), end-to-end distance, maximum distance (backbone only), intramolecular hydrogen bonds, and hydrogen bonds with water for each compositionally identical sequence. b) Representations of the highest abundance conformations from clustering each of the model sequences (1.4 Å cut-off). c) Probability densities depicting the radius of gyration (backbone only) versus end-to-end distance highlighting the range of individual conformations for each of the four sequences.

To complement measures of radius, the 50,000 conformations were clustered by conformational similarity (within a backbone RMSD of 1.4 Å). This analysis revealed that **alt** has the fewest accessible conformations with 6954 clusters and **r1** had 8275 (Table S2), while conformations for **r2** were grouped into 10813 clusters of similar conformations and **dib** into 14385. This comparison reveals that **alt** has half the number of clusters as **dib**, thus the ensemble of conformations of the diblock included significantly more conformational disorder. The highest abundance conformations are illustrated in Figures 3b and S3,4. The differences in the full conformational distribution are most visually apparent when plotting a probability distribution of $R_{g(bkb)}$ and R_{ee} (Figures 3c and S5), where more abundant regions are observed for **alt**, followed by **r1**, with less clustering apparent in **r2** and **dib**. The hydrophobic region formed by these macromolecules facilitates environments for intramolecular hydrogen bonds, minimizing hydrogen bonds formed with water. Of the four sequences, **alt** on average had more intramolecular hydrogen bonds (Figure 3a) and fewer hydrogen bonds with water than the other three compositionally identical peptoids (Figure 3a and Table S3). From these collective measurements of the simulated peptoids, we conclude that **alt** is the most compact, followed by **r1** and then **r2**, and **dib** is the most disordered of the four peptoids.

Experimental characterization of peptoid sequences. While atomistic simulations offer detailed information at atomic-level resolution, complementary experimental techniques were employed to validate the analysis and to identify more rapid characterization strategies. Well-established techniques to characterize differences in molecular size and structure for small macromolecules (the model peptoids each have a molecular weight of 1719 g/mol) include ion mobility spectrometry (IMS), NMR spectroscopy, and end-to-end distance measurements with double electron-electron resonance (DEER) spectroscopy. We synthesized and experimentally characterized **alt**, **r1**, and **r2**, omitting **dib** due to the propensity of this architecture to aggregate in solution.[32,51]

IMS, typically coupled with liquid chromatography and mass spectrometry (LC-MS) in complex sample analyses, is a powerful tool for resolving small structural differences. IMS has differentiated disordered polymer architectures[13] and charge placement in a series of three compositionally identical oligomeric peptoids.[28] Characterization of purified model peptoids (Figure S6-7) with IMS revealed that **alt** was the most compact with a collisional cross-section (CCS) of 460.4 ± 0.5 Å^2 (Figure 4a, S8), in agreement with simulations. Statistically indistinguishable CCS measurements were observed for **r1** and **r2**, 461.7 ± 0.5 Å^2 and 462.2 ± 0.5 Å^2, respectively. Interestingly, we observed that **alt** eluted earliest on the LC chromatogram (9.60 ± 0.02 min) compared to **r1** and **r2** (9.63 ± 0.02 and 9.70 ± 0.03 min, respectively). While retention time on reversed phase columns is indicative of molecule polarity, branched small molecules have been observed to elute earlier via LC than their linear isomers with a larger surface area, highlighting that isomers can have different retention times.[52] Evaluating both LC and IMS, **r2** had a longer retention and larger CCS value, data consistent with the conclusion from the simulations that **r2** is more disordered than **r1** and **alt** (Figure 4a).

Since these peptoid sequences contain a distribution of conformations as opposed to a single crystalline folded structure, we anticipated that conformational differences would be challenging to observe experimentally and were excited to see the combination of retention time and CCS recapitulated trends observed in the simulations. Of note, both LC and IMS are performed in non-native environments (e.g., organic and gas phase). As each of the selected model sequences contain the same composition and conformations are driven by hydrophobic interactions, we hypothesize that conformational differences are maintained in these different environments.

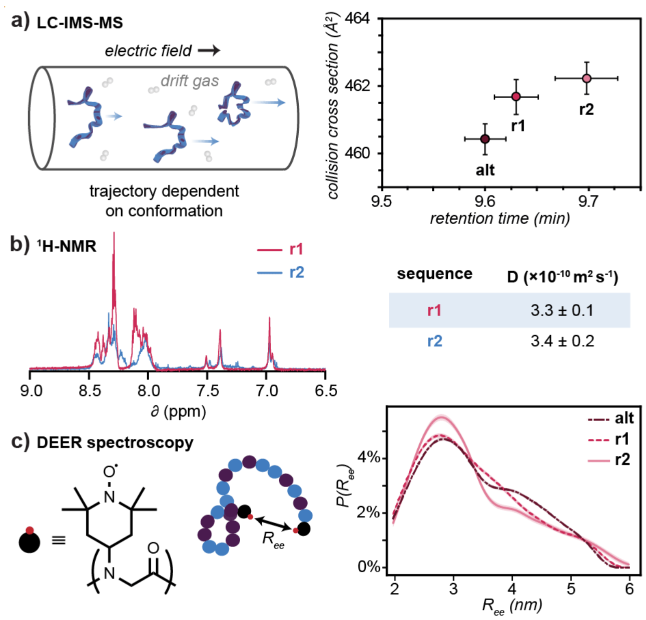

Figure 4. Experimental analysis of peptoids. a) Ion mobility spectrometry including a schematic (left) and a plot of reversed phase liquid chromatography retention time and collisional cross-section from ion mobility spectrometry (right). Error bars represent standard deviation of multiple runs (n = 5). b) ^{1}H-NMR characterization of the amide region of ^{1}H-NMR of non-aggregating peptoids **r1** and **r2** and the diffusion coefficients calculated with DOSY (right). c) End-to-end distance characterization with DEER including a schematic of the introduction of radical probes into the peptoids (left) and the probability distributions of end-to-end distances resulting from DEER spectroscopy measurements.

To probe conformational differences in a native environment, diffusion ordered spectroscopy (DOSY) was employed, as it has been used to analyze mixtures of biomolecules by molecular diffusivity[12] and to characterize structural distinctions of peptides and foldamers.[53,54] Purified model sequences (0.5 mM) were prepared in acetate buffer (50 mM, pH 4.5). While **r1** and **r2** were amenable to NMR characterization under these solution conditions, we were unable to observe strong signals for **alt** by ^{1}H-NMR. This is likely due to extreme line broadening caused by aggregation, which was visually observable at high concentrations (Figure S9). The diffusion coefficients for the remaining two 20mer peptoids did not suggest significant differences in macromolecular size (Figures 4b and S10). However, there were differences in the ^{1}H-NMR spectrum (Figures 4b and S11). These differences can be caused by unique monomer connectivity and conformationally dependent solvent accessibility and through-space interactions.

Another method for studying native conformation is through the addition of molecular probes for site-specific distance measurements. Radical probes within a protein or polymer have been used to measure distances between two specific residues.[14,55,56] For the first and last residues of each target peptoid, 4-amino-TEMPO, a radical source, was introduced using the submonomer synthetic method (Figure S12-14).[57] The radicals were reintroduced with ammonia as they were quenched by trifluoroacetic acid during the resin cleavage. As measured by DEER spectroscopy, the average R_{ee} distance distributions were not differentiable for the three model peptoids (3.40, 3.34, and 3.34 nm for **alt**, **r1**, and **r2**, respectively; Figures 4c and S15). However, DEER provides high resolution measurements ranging from 2-9 nm, and structures within the population that are outside of the specified range are not observed.[14] These data are consistent with the simulation results that the macromolecules are compact with end-to-end distances below 2 nm for most conformations, and the addition of TEMPO probes will not significantly increase the diameter.

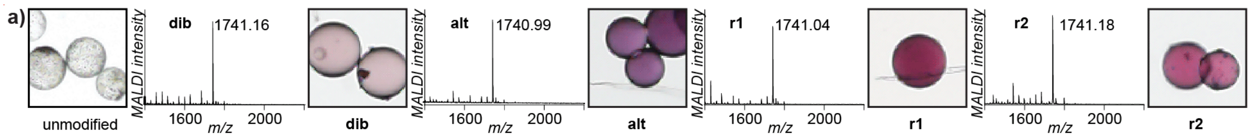

b)

sequence	dye saturation	$R_{g\,(bkb)}$	$R_{max\,(bkb)}$ (nm)	R_{ee}	# hydrogen bonds intramolecular	water	# clusters	LC-IMS-MS RT (min)	CCS (Å²)	diffusion (×10⁻¹⁰ m² s⁻¹) excluding amide	DEER-EPR average (nm)	median (nm)
alt	darkest	0.623	1.81	1.16	3.40	22.2	6954	9.60 ± 0.02	460.4 ± 0.5	---	3.40	3.25
r1		0.631	1.83	1.23	3.19	23.0	8275	9.63 ± 0.02	461.7 ± 0.5	3.3 ± 0.1	3.34	3.17
r2		0.652	1.95	1.39	2.83	24.0	10813	9.70 ± 0.03	462.2 ± 0.5	3.4 ± 0.2	3.33	3.08
dib	palest	0.645	1.88	1.25	3.10	23.4	14385	---	---	---	---	---

Figure 5. Immobilized colorimetric assay: a) PEGA resin incubated with Reichardt's dye (0.150 mM in 100 HEPES pH = 7.8) imaged on brightfield microscope, and respective MALDI-TOF MS spectra of cleaved material for each of the four peptoid sequences, and b) comparisons across all characterization methods, including average measurements from the atomistic simulations.

Immobilized colorimetric assay. While these computational and experimental techniques are information rich, they can be time- and resource-intensive, require access to specialized instrumentation and associated expertise, or may not be able to resolve conformational differences at small size scales (< 3 kDa). We hypothesized that a solvatochromic dye could provide a facile self-consistent qualitative assessment of macromolecule conformation to complement the techniques previously described. Further, the assay could be implemented on the solid-phase resin required for synthesis, eliminating both the potential for multi-chain aggregation and the need for resin cleavage. Immobilized strategies have been used in high-throughput screens of ligands[58,59] and for assays probing single chain structure with atomic force microscopy.[60] Reichardt's dye[61] was chosen as a conformational probe due to the rapid one-step synthesis[62] (Figure S16) and desirable water insolubility, reducing any background signal. Further, the dye exhibits vibrant colors upon introduction to a hydrophobic environment.[33] The four model peptoids were synthesized on a poly(acrylamide) resin crosslinked with poly(ethylene glycol) (PEGA), which is a water-swellable support that demonstrates no interaction with Reichardt's dye when unfunctionalized (Figure 5a). Each bead of resin is 50-100 µm in diameter and contains many spatially separated copies of a single sequence. PEGA resin has shown to be permeable by molecules >35 kDa, indicating a significant pore size.[63,64] To confirm high-purity synthesis on the PEGA resin, a portion of the resin was cleaved and characterized via LC-MS and MALDI-TOF MS (Figure 5a and S17-18).

The peptoid-functionalized resin was incubated with a buffered solution of Reichardt's dye (0.15 mM in 100 mM HEPES, pH 7.8). The color of the resin was visualized with optical microscopy and was observed to correlate with the previously identified conformational trends. Reichardt's dye is better solubilized by more hydrophobic environments, and thus we hypothesized that darker colors would correspond to more hydrophobic pockets formed by a more compact peptoid.[38,39] The resin color was consistent across beads of different diameters, suggesting the bead size distribution did not affect the colorimetric output (Figure 5a). The darkest color was observed for **alt,** correlating with the more compact structure consistent with observations from simulations and LC-IMS-MS (Figure 5b). The paler color of **dib** correlates with the most disordered structure, correlating with simulations. The randomized sequences were intermediate in dye saturation with **r1** darker than **r2**, consistent with observations from LC-IMS-MS and simulations that characterize **r2** as more disordered than **r1**. The dye saturation showed slight variations in replicate preparations and under different cameras; however, the color intensity trends remained the same across the peptoid sequences (Figures S19-20). Thus, this immobilized system enables facile analysis of small differences between conformational ensembles in a semi-quantitative colorimetric fashion, without requiring specialized instrumentation or expertise.

Conclusion

Disordered peptidomimetics provide a fruitful platform for developing functional materials, but their broad conformational ensembles can present challenges for characterization. A combination of complementary characterization techniques therefore becomes essential for studying small, disordered oligomers, as each technique provides unique descriptors regarding the composition of the conformational ensemble. This is especially pertinent for compositionally identical macromolecules, exemplified by the four peptoids investigated in this study. Through the integration of atomistic simulations and IMS coupled to LC, our data reveals a diverse range of distinct conformational ensembles accessible to compositionally identical peptoids. Notably, these conformational trends correlate with the colorimetric output of a Reichardt's dye assay, which requires no specialized instrumentation or expertise. By utilizing these techniques in combination, we can thus discern even subtle differences in conformation, as the complementary conformational descriptors increase confidence in these nuanced results. Interestingly, we observed that the alternating conformation was the most compact. This finding underscores a key point: while randomized sequences can access more compact conformations than regular patterns,[30] our results demonstrate the necessity of specific hydrophobic patterns for achieving this compactness.

Exploring additional sequences with the suite of techniques described herein will yield valuable structural insights and facilitate connections between sequence, structure, and function. The colorimetric assay and LC-IMS-MS analysis will benefit from ongoing comparisons to simulations, NMR spectroscopy, and end-to-end distance measurements to elucidate molecular mechanisms. The resolution of DEER and DOSY spectroscopies can be enhanced in future efforts by increasing the radical concentration and incorporating isotopic probes, respectively.

Further expansion of the colorimetric assay will offer additional inexpensive and accessible methods for studying conformational differences in peptidomimetics and foldamers. The use of motif specific dyes (e.g., Thioflavin T for β-sheets[65]) would expand the applicability and specificity of this system beyond disordered collapse. Additionally, this assay can be completed in high throughput followed by corroboration with specialized lower-throughput techniques. This allows for the rapid analysis of the impact of varying environmental conditions on conformational distributions (e.g., solvent or salt variations) in addition to combination with existing immobilized assays. Continued elucidation of conformational descriptors will inform the design of macromolecules with desired properties that can be equipped with functional handles, paving the way for tailored functional materials, receptors, and therapeutics.

Author information

Corresponding Author

* Abigail S. Knight – Department of Chemistry, The University of North Carolina at Chapel Hill, Chapel Hill, North Carolina 27599, United States; https://orcid.org/0000-0003-1524-473X Email: aknight@unc.edu

Authors

Erin C. Day – Department of Chemistry, The University of North Carolina at Chapel Hill, Chapel Hill, North Carolina 27599, United States; https://orcid.org/0000-0001-9278-9560

Keila C. Cunha: Department of Chemistry and Biochemistry, University of California, Santa Barbara, Santa Barbara, California 93106, United States

Jianhan Zhao: Department of Physics & Astronomy, University of California, Los Angeles, Los Angeles, California 90095, United States; https://orcid.org/0009-0001-9716-4188

Audra J. DeStefano: Department of Chemical Engineering, University of California, Santa Barbara, California 93106, United States; https://orcid.org/0000-0003-1047-2637

James N. Dodds: Department of Chemistry, The University of North Carolina at Chapel Hill, Chapel Hill, North Carolina 27599, United States; https://orcid.org/0000-0002-9702-2294

Melissa A. Yu: Department of Chemistry, The University of North Carolina at Chapel Hill, Chapel Hill, North Carolina 27599, United States

Songi Han: Department of Chemistry and Biochemistry and Department of Chemical Engineering, University of California, Santa Barbara, Santa Barbara, California 93106, United States; https://orcid.org/0000-0001-6489-6246

Erin S. Baker: Department of Chemistry, The University of North Carolina at Chapel Hill, Chapel Hill, North Carolina 27599, United States; https://orcid.org/0000-0001-5246-2213

Joan-Emma Shea: Department of Chemistry and Biochemistry and Department of Physics, University of California, Santa Barbara, Santa Barbara, California 93106, United States; https://orcid.org/0000-0002-9801-9273

Rebecca B. Berlow: Department of Biochemistry and Biophysics and Lineberger Comprehensive Cancer Center, The University of North Carolina at Chapel Hill, Chapel Hill, North Carolina 27599, United States; https://orcid.org/0000-0003-1934-0139

Acknowledgment

This material is based upon experimental work (A.S.K.) supported by the Air Force Office of Scientific Research under Award Number FA9550-20-1-0172. E.C.D. and A.J.D. acknowledge support from the National Defense Science & Engineering Graduate (NDSEG) Fellowship Program and J.N.D and E.S.B acknowledge support from the National Institute of Environmental Health Sciences (P42 ES027704), the National Institute of General Medical Sciences (RM1 GM145416) and a cooperative agreement with the U.S. Environmental Protection Agency (STAR RD 84003201). R.B.B. gratefully acknowledges institutional support from the Department of Biochemistry and Biophysics and the Dean's Office at the UNC School of Medicine as well as the Lineberger Comprehensive Cancer Center. We acknowledge the NMR core laboratory supported by a National Science Foundation award number CHE-1828183 and the UNC peptide synthesis core facility (RRID:SCR_017837). We additionally thank Stuart Parnham for expert advice on experimental design and the Biomolecular NMR Laboratory which receives funding from the National Cancer Institute of the National Institutes of Health under award number P30CA016086. J.E.S. acknowledges support from the Center for Scientific Computing at the California Nanosystems Institute (CNSI, NSF grant CNS-1725797). This work (J.E.S.) used the Extreme Science and Engineering Discovery Environment, which is supported by the National Science Foundation grant ACI-1548562 (MCA05S027). J.E.S. acknowledges support from the NSF (MCB-1716956). This work (J.E.S.) was partially supported by the National Science Foundation through the Materials Research Science and Engineering Center (MRSEC) at UC Santa Barbara: NSF DMR–2308708 (IRG-2). S.H. thanks the National Institute of General Medicine grant (R35GM136411) for method development support.

Abbreviations

CCS, collisional cross-section; DEER, double electron-electron resonance; DOSY, diffusion ordered spectroscopy; IMS, ion mobility spectrometry; kDa, kilodalton; LC-MS, liquid chromatography and mass spectrometry; MALDI-TOF, matrix assisted laser desorption ionization time of flight spectrometry; MD, molecular dynamics; NMR, nuclear magnetic resonance; PEGA, poly(ethylene glycol) crosslinked acrylamide; RMSD, root mean square deviation; TEMPO, (2,2,6,6-tetramethylpiperidin-1-yl)oxyl.

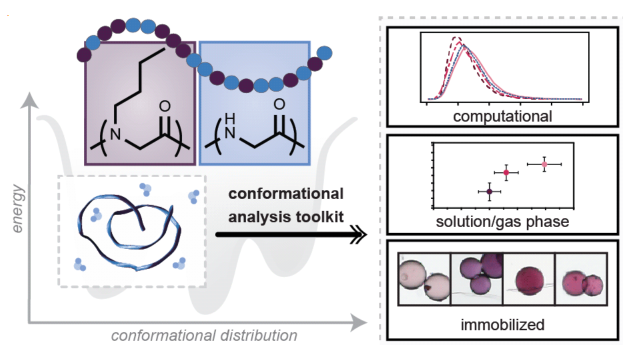

References

(1) Fowler, S. A.; Blackwell, H. E. Structure-Function Relationships in Peptoids: Recent Advances toward Deciphering the Structural Requirements for Biological Function. *Organic and Biomolecular Chemistry* **2009**, *7* (8), 1508–1524. https://doi.org/10.1039/b817980h.

(2) Van Der Lee, R.; Buljan, M.; Lang, B.; Weatheritt, R. J.; Daughdrill, G. W.; Dunker, A. K.; Fuxreiter, M.; Gough, J.; Gsponer, J.; Jones, D. T.; Kim, P. M.; Kriwacki, R. W.; Oldfield, C. J.; Pappu, R. V.; Tompa, P.; Uversky, V. N.; Wright, P. E.; Babu, M. M. Classification of Intrinsically Disordered Regions and Proteins. *Chemical Reviews* **2014**, *114* (13), 6589–6631. https://doi.org/10.1021/cr400525m.

(3) Dill, K. A.; MacCallum, J. L. The Protein-Folding Problem, 50 Years On. *Science* **2012**, *338* (6110), 1042–1046. https://doi.org/10.1126/science.1219021.

(4) Kuhlman, B.; Bradley, P. Advances in Protein Structure Prediction and Design. *Nat Rev Mol Cell Biol* **2019**, *20* (11), 681–697. https://doi.org/10.1038/s41580-019-0163-x.

(5) Baker, E. G.; Bartlett, G. J.; Porter Goff, K. L.; Woolfson, D. N. Miniprotein Design: Past, Present, and Prospects. *Accounts of Chemical Research* **2017**, *50* (9), 2085–2092. https://doi.org/10.1021/acs.accounts.7b00186.

(6) Yang, C.; Wu, K. B.; Deng, Y.; Yuan, J.; Niu, J. Geared Toward Applications: A Perspective on Functional Sequence-Controlled Polymers. *ACS Macro Lett.* **2021**, *10*, 243–257. https://doi.org/10.1021/acsmacrolett.0c00855.

(7) DeStefano, A. J.; Segalman, R. A.; Davidson, E. C. Where Biology and Traditional Polymers Meet: The Potential of Associating Sequence-Defined Polymers for Materials Science. *JACS Au* **2021**, *1* (10), 1556–1571. https://doi.org/10.1021/jacsau.1c00297.

(8) Hara, T.; Durell, S. R.; Myers, M. C.; Appella, D. H. Probing the Structural Requirements of Peptoids That Inhibit HDM2−p53 Interactions. *J. Am. Chem. Soc.* **2006**, *128* (6), 1995–2004. https://doi.org/10.1021/ja056344c.

(9) Warren, J. L.; Dykeman-Bermingham, P. A.; Knight, A. S. Controlling Amphiphilic Polymer Folding beyond the Primary Structure with Protein-Mimetic Di(Phenylalanine). *Journal of the American Chemical Society* **2021**, *143* (33), 13228–13234. https://doi.org/10.1021/JACS.1C05659.

(10) *Circular Dichroism: Principles and Applications*; Nakanishi, K., Berova, N., Woody, R., Eds.; VCH: New York, N.Y, 1994.

(11) Bakshi, K.; Liyanage, M. R.; Volkin, D. B.; Middaugh, C. R. Fourier Transform Infrared Spectroscopy of Peptides. In *Therapeutic Peptides*; Nixon, A. E., Ed.; Methods in Molecular Biology; Humana Press: Totowa, NJ, 2014; Vol. 1088, pp 255–269. https://doi.org/10.1007/978-1-62703-673-3_18.

(12) Johnson, C. S. Diffusion Ordered Nuclear Magnetic Resonance Spectroscopy: Principles and Applications. *Progress in Nuclear Magnetic Resonance Spectroscopy* **1999**, *34* (3–4), 203–256. https://doi.org/10.1016/S0079-6565(99)00003-5.

(13) Foley, C. D.; Zhang, B.; Alb, A. M.; Trimpin, S.; Grayson, S. M. Use of Ion Mobility Spectrometry-Mass Spectrometry to Elucidate Architectural Dispersity within Star Polymers. *ACS Macro Letters* **2015**, *4* (7), 778–782. https://doi.org/10.1021/acsmacrolett.5b00299.

(14) Jiao, S.; DeStefano, A.; Monroe, J. I.; Barry, M.; Sherck, N.; Casey, T.; Segalman, R. A.; Han, S.; Shell, M. S. Quantifying Polypeptoid Conformational Landscapes through Integrated Experiment and Simulation. *Macromolecules* **2021**, *54* (11), 5011–5021. https://doi.org/10.1021/acs.macromol.1c00550.

(15) Barbee, M. H.; Wright, Z. M.; Allen, B. P.; Taylor, H. F.; Patteson, E. F.; Knight, A. S. Protein-Mimetic Self-Assembly with Synthetic Macromolecules. *Macromolecules* **2021**, *54* (8), 3585–3612. https://doi.org/10.1021/acs.macromol.0c02826.

(16) Rosales, A. M.; Segalman, R. A.; Zuckermann, R. N. Polypeptoids: A Model System to Study the Effect of Monomer Sequence on Polymer Properties and Self-Assembly. *Soft Matter* **2013**, *9* (35), 8400–8414. https://doi.org/10.1039/c3sm51421h.

(17) Godballe, T.; Nilsson, L. L.; Petersen, P. D.; Jenssen, H. Antimicrobial β-Peptides and α-Peptoids: Antimicrobial Peptidomimetics. *Chemical Biology & Drug Design* **2011**, *77* (2), 107–116. https://doi.org/10.1111/j.1747-0285.2010.01067.x.

(18) Zuckermann, R. N.; Kodadek, T. Peptoids as Potential Therapeutics. *Curr Opin Mol Ther* **2009**, *11* (3), 299–307.

(19) Girvin, Z. C.; Gellman, S. H. Foldamer Catalysis. *J. Am. Chem. Soc.* **2020**, *142* (41), 17211–17223. https://doi.org/10.1021/jacs.0c07347.

(20) Legrand, B.; Aguesseau-Kondrotas, J.; Simon, M.; Maillard, L. Catalytic Foldamers: When the Structure Guides the Function. *Catalysts* **2020**, *10* (6), 1–20. https://doi.org/10.3390/catal10060700.

(21) Leguizamon, S. C.; Scott, T. F. Sequence-Selective Dynamic Covalent Assembly of Information-Bearing Oligomers. *Nature Communications* **2020**, *11* (1), 784. https://doi.org/10.1038/s41467-020-14607-3.

(22) Prince, R. B.; Barnes, S. A.; Moore, J. S. Foldamer-Based Molecular Recognition. *J. Am. Chem. Soc.* **2000**, *122* (12), 2758–2762. https://doi.org/10.1021/ja993830p.

(23) Behar, A. E.; Maayan, G. The First Cu(I)-Peptoid Complex: Enabling Metal Ion Stability and Selectivity via Backbone Helicity. *Chemistry A European J* **2023**, e202301118. https://doi.org/10.1002/chem.202301118.

(24) Olivier, G. K.; Cho, A.; Sanii, B.; Connolly, M. D.; Tran, H.; Zuckermann, R. N. Antibody-Mimetic Peptoid Nanosheets for Molecular Recognition. *ACS Nano* **2013**, *7* (10), 9276–9286. https://doi.org/10.1021/nn403899y.

(25) Rzeigui, M.; Traikia, M.; Jouffret, L.; Kriznik, A.; Khiari, J.; Roy, O.; Taillefumier, C. Strengthening Peptoid Helicity through Sequence Site-Specific Positioning of Amide Cis -Inducing Nt Bu Monomers. *The Journal of Organic Chemistry* **2020**, *85* (4), 2190–2201. https://doi.org/10.1021/acs.joc.9b02916.

(26) Davidson, E. C.; Rosales, A. M.; Patterson, A. L.; Russ, B.; Yu, B.; Zuckermann, R. N.; Segalman, R. A. Impact of Helical Chain Shape in Sequence-Defined Polymers on Polypeptoid Block Copolymer Self-Assembly. *Macromolecules* **2018**, *51* (5), 2089–2098. https://doi.org/10.1021/acs.macromol.8b00055.

(27) Hoyas, S.; Halin, E.; Lemaur, V.; De Winter, J.; Gerbaux, P.; Cornil, J. Helicity of Peptoid Ions in the Gas Phase. *Biomacromolecules* **2020**, *21* (2), 903–909. https://doi.org/10.1021/acs.biomac.9b01567.

(28) Weber, P.; Hoyas, S.; Halin, É.; Coulembier, O.; De Winter, J.; Cornil, J.; Gerbaux, P. On the Conformation of Anionic Peptoids in the Gas Phase. *Biomacromolecules* **2022**, acs.biomac.1c01442. https://doi.org/10.1021/acs.biomac.1c01442.

(29) Sanii, B.; Kudirka, R.; Cho, A.; Venkateswaran, N.; Olivier, G. K.; Olson, A. M.; Tran, H.; Harada, R. M.; Tan, L.; Zuckermann, R. N. Shaken, Not Stirred: Collapsing a Peptoid Monolayer to Produce Free-Floating, Stable Nanosheets. *Journal of the American Chemical Society* **2011**, *133* (51), 20808–20815. https://doi.org/10.1021/ja206199d.

(30) Murnen, H. K.; Khokhlov, A. R.; Khalatur, P. G.; Segalman, R. A.; Zuckermann, R. N. Impact of Hydrophobic Sequence Patterning on the Coil-to-Globule Transition of Protein-like Polymers. *Macromolecules* **2012**, *45* (12), 5229–5236. https://doi.org/10.1021/ma300707t.

(31) Patterson, A. L.; Yu, B.; Danielsen, S. P. O.; Davidson, E. C.; Fredrickson, G. H.; Segalman, R. A. Monomer Sequence Effects on Interfacial Width and Mixing in Self-Assembled Diblock Copolymers. *Macromolecules* **2020**, acs.macromol.9b02426. https://doi.org/10.1021/acs.macromol.9b02426.

(32) Sternhagen, G. L.; Gupta, S.; Zhang, Y.; John, V.; Schneider, G. J.; Zhang, D. Solution Self-Assemblies of Sequence-Defined Ionic Peptoid Block Copolymers. *Journal of the American Chemical Society* **2018**, *140* (11), 4100–4109. https://doi.org/10.1021/jacs.8b00461.

(33) Reichardt, C. Solvatochromic Dyes as Solvent Polarity Indicators. *Chemical Reviews* **1994**, *94* (8), 2319–2358. https://doi.org/10.1021/cr00032a005.

(34) Sackett, D. L.; Wolff, J. Nile Red as a Polarity-Sensitive Fluorescent Probe of Hydrophobic Protein Surfaces. *Analytical Biochemistry* **1987**, *167* (2), 228–234. https://doi.org/10.1016/0003-2697(87)90157-6.

(35) Greenspan, P.; Mayer, E. P.; Fowler, S. D. Nile Red: A Selective Fluorescent Stain for Intracellular Lipid Droplets. *The Journal of Cell Biology* **1985**, *100* (3), 965–973. https://doi.org/10.1083/jcb.100.3.965.

(36) Li, Q.; Zhang, H.; Lou, K.; Yang, Y.; Ji, X.; Zhu, J.; Sessler, J. L. Visualizing Molecular Weights Differences in Supramolecular Polymers. *Proceedings of the National Academy of Sciences* **2022**, *119* (9), 1–9. https://doi.org/10.1073/pnas.2121746119.

(37) Pan, Y.; Ford, W. T. Dendrimers with Both Hydrophilic and Hydrophobic Chains at Every End. *Macromolecules* **1999**, *32* (16), 5468–5470. https://doi.org/10.1021/ma990675q.

(38) Macquarrie, D. J.; Tavener, S. J.; Gray, G. W.; Heath, P. A.; Rafelt, J. S.; Saulzet, S. I.; Hardy, J. J. E.; Clark, J. H.; Sutra, P.; Brunel, D.; Di Renzo, F.; Fajula, F. The Use of Reichardt's Dye as an Indicator of Surface Polarity. *New Journal of Chemistry* **1999**, *23* (7), 725–731. https://doi.org/10.1039/a901563i.

(39) Terashima, T.; Sugita, T.; Fukae, K.; Sawamoto, M. Synthesis and Single-Chain Folding of Amphiphilic Random Copolymers in Water. *Macromolecules* **2014**, *47* (2), 589–600. https://doi.org/10.1021/ma402355v.

(40) Fetsch, C.; Flecks, S.; Gieseler, D.; Marschelke, C.; Ulbricht, J.; van Pée, K.-H.; Luxenhofer, R. Self-Assembly of Amphiphilic Block Copolypeptoids with C 2 -C 5 Side Chains in Aqueous Solution. *Macromolecular Chemistry and Physics* **2015**, *216* (5), 547–560. https://doi.org/10.1002/macp.201400534.

(41) Varadaraj, R.; Bock, J.; Valint, P.; Brons, N. Micropolarity and Water Penetration in Micellar Aggregates of Linear and Branched Hydrocarbon Surfactants. *Langmuir* **1990**, *6* (8), 1376–1378. https://doi.org/10.1021/la00098a010.

(42) Varadaraj, R.; Bock, J.; Brons, N.; Pace, S. Probing Hydrophobic Microdomains of Hydrophobically Associating Acrylamide-N-Alkylacrylamide Copolymers in Solution Using a Solvatochromic Absorption Dye Probe. *The Journal of Physical Chemistry* **1993**, *97* (49), 12991–12994. https://doi.org/10.1021/j100151a056.

(43) Ashbaugh, H. S. Tuning the Globular Assembly of Hydrophobic/Hydrophilic Heteropolymer Sequences. *Journal of Physical Chemistry B* **2009**, *113* (43), 14043–14046. https://doi.org/10.1021/jp907398r.

(44) Guseva, E.; Zuckermann, R. N.; Dill, K. A. Foldamer Hypothesis for the Growth and Sequence Differentiation of Prebiotic Polymers. *Proceedings of the National Academy of Sciences* **2017**, *114* (36), E7460–E7468. https://doi.org/10.1073/pnas.1620179114.

(45) Faizullina, K.; Burovski, E. Globule-Coil Transition in the Dynamic HP Model. *Journal of Physics: Conference Series* **2021**, *1740* (1). https://doi.org/10.1088/1742-6596/1740/1/012014.

(46) Gellman, S. H. Foldamers: A Manifesto. *Accounts of Chemical Research* **1998**, *31* (4), 173–180. https://doi.org/10.1021/ar960298r.

(47) Ihsan, A. B.; Koyama, Y. Impact of Polypeptide Sequence on Thermal Properties for Diblock, Random, and Alternating Copolymers Containing a Stoichiometric Mixture of Glycine and Valine. *Polymer* **2019**, *161* (December 2018), 197–204. https://doi.org/10.1016/j.polymer.2018.12.021.

(48) Ruan, Z.; Li, S.; Grigoropoulos, A.; Amiri, H.; Hilburg, S. L.; Chen, H.; Jayapurna, I.; Jiang, T.; Gu, Z.; Alexander-Katz, A.; Bustamante, C.; Huang, H.; Xu, T. Population-Based Heteropolymer Design to Mimic Protein Mixtures. *Nature* **2023**, *615* (7951), 251–258. https://doi.org/10.1038/s41586-022-05675-0.

(49) Zuckermann, R. N.; Kerr, J. M.; Moos, W. H.; Kent, S. B. H. Efficient Method for the Preparation of Peptoids [Oligo(N-Substituted Glycines)] by Submonomer Solid-Phase Synthesis. *Journal of the American Chemical Society* **1992**, *114* (26), 10646–10647. https://doi.org/10.1021/ja00052a076.

(50) Wonderly, W. R.; Cristiani, T. R.; Cunha, K. C.; Degen, G. D.; Shea, J.; Waite, J. H. Dueling Backbones: Comparing Peptoid and Peptide Analogues of a Mussel Adhesive Protein. *Macromolecules* **2020**, *53* (16), 6767–6779. https://doi.org/10.1021/acs.macromol.9b02715.

(51) DeStefano, A. J.; Nguyen, M.; Fredrickson, G. H.; Han, S.; Segalman, R. A. Design of Soft Material Surfaces with Rationally Tuned Water Diffusivity. *ACS Cent. Sci.* **2023**, acscentsci.3c00208. https://doi.org/10.1021/acscentsci.3c00208.

(52) Dodds, J. N.; Hopkins, Z. R.; Knappe, D. R. U.; Baker, E. S. Rapid Characterization of Per- and Polyfluoroalkyl Substances (PFAS) by Ion Mobility Spectrometry–Mass Spectrometry (IMS-MS). *Anal. Chem.* **2020**, *92* (6), 4427–4435. https://doi.org/10.1021/acs.analchem.9b05364.

(53) Schwartz, A. C.; Jay, D. W.; Parnham, S.; Giuliano, M. W. Sequential and Environmental Dependence of Conformation in a Small Opioid Peptide. *J. Org. Chem.* **2019**, *84* (21), 13299–13312. https://doi.org/10.1021/acs.joc.9b01141.

(54) Wang, S.; Della Sala, F.; Cliff, M. J.; Whitehead, G. F. S.; Vitórica-Yrezábal, I. J.; Webb, S. J. A Chiral ^{19}F NMR Reporter of Foldamer Conformation in Bilayers. *J. Am. Chem. Soc.* **2022**, *144* (47), 21648–21657. https://doi.org/10.1021/jacs.2c09103.

(55) Sahu, I. D.; McCarrick, R. M.; Troxel, K. R.; Zhang, R.; Smith, H. J.; Dunagan, M. M.; Swartz, M. S.; Rajan, P. V.; Kroncke, B. M.; Sanders, C. R.; Lorigan, G. A. DEER EPR Measurements for Membrane Protein Structures via Bifunctional Spin Labels and Lipodisq Nanoparticles. *Biochemistry* **2013**, *52* (38), 6627–6632. https://doi.org/10.1021/bi4009984.

(56) Sherck, N.; Webber, T.; Brown, D. R.; Keller, T.; Barry, M.; DeStefano, A.; Jiao, S.; Segalman, R. A.; Fredrickson, G. H.; Shell, M. S.; Han, S. End-to-End Distance Probability Distributions of Dilute Poly(Ethylene Oxide) in Aqueous Solution. *J. Am. Chem. Soc.* **2020**, 11.

(57) Connolly, M. D.; Xuan, S.; Molchanova, N.; Zuckermann, R. N. *Submonomer Synthesis of Sequence Defined Peptoids with Diverse Side-Chains*; Elsevier Inc., 2021; Vol. 656. https://doi.org/10.1016/bs.mie.2021.04.022.

(58) Knight, A. S.; Zhou, E. Y.; Pelton, J. G.; Francis, M. B. Selective Chromium(VI) Ligands Identified Using Combinatorial Peptoid Libraries. *Journal of the American Chemical Society* **2013**, *135* (46), 17488–17493. https://doi.org/10.1021/ja408788t.

(59) Alluri, P. G.; Reddy, M. M.; Bachhawat-Sikder, K.; Olivos, H. J.; Kodadek, T. Isolation of Protein Ligands from Large Peptoid Libraries. *J. Am. Chem. Soc.* **2003**, *125* (46), 13995–14004. https://doi.org/10.1021/ja036417x.

(60) Ma, C. D.; Acevedo-Vélez, C.; Wang, C.; Gellman, S. H.; Abbott, N. L. Interaction of the Hydrophobic Tip of an Atomic Force Microscope with Oligopeptides Immobilized Using Short and Long Tethers. *Langmuir* **2016**, *32* (12), 2985–2995. https://doi.org/10.1021/acs.langmuir.5b04618.

(61) Dimroth, K.; Reichardt, C.; Siepmann, T.; Bohlmann, F. Über Pyridinium-N-phenol-betaine und ihre Verwendung zur Charakterisierung der Polarität von Lösungsmitteln. *Justus Liebigs Ann. Chem.* **1963**, *661* (1), 1–37. https://doi.org/10.1002/jlac.19636610102.

(62) Osterby, B. R.; McKelvey, R. D. Convergent Synthesis of Betaine-30, a Solvatochromic Dye: An Advanced Undergraduate Project and Demonstration. *J. Chem. Educ.* **1996**, *73* (3), 260. https://doi.org/10.1021/ed073p260.

(63) Kress, J.; Zanaletti, R.; Amour, A.; Ladlow, M.; Frey, J. G.; Bradley, M. Enzyme Accessibility and Solid Supports: Which Molecular Weight Enzymes Can Be Used on Solid Supports? An Investigation Using Confocal Raman Microscopy. *Chem. Eur. J.* **2002**, *8* (16), 3769. https://doi.org/10.1002/1521-3765(20020816)8:16<3769::AID-CHEM3769>3.0.CO;2-V.

(64) Meldal, M. Pega: A Flow Stable Polyethylene Glycol Dimethyl Acrylamide Copolymer for Solid Phase Synthesis. *Tetrahedron Letters* **1992**, *33* (21), 3077–3080. https://doi.org/10.1016/S0040-4039(00)79604-3.

(65) Wu, C.; Biancalana, M.; Koide, S.; Shea, J. E. Binding Modes of Thioflavin-T to the Single-Layer β-Sheet of the Peptide Self-Assembly Mimics. *Journal of Molecular Biology* **2009**, *394* (4), 627–633. https://doi.org/10.1016/j.jmb.2009.09.056.